A magneto-reflectivity study of $CuInTe_2$ single crystals

Michael V. Yakushev,[1,2,3,4*] Clement Faugeras, [5] Alexander V. Mudryi,[6] and Robert W. Martin[1]

[1] Department of Physics, SUPA, Strathclyde University, G4 0NG Glasgow, UK.
[2] M.N. Miheev Institute of Metal Physics of the UB RAS, 18 S. Kovalevskoy St. 620108, Ekaterinburg, Russia.
[3] Ural Federal University, 19 Mira St., 620002 Ekaterinburg, Russia.
[4] Institute of Solid State Chemistry of the Urals branch of the Russian Academy of Sciences, Ekaterinburg, 620990, Russia.
[5] LNCMI-CNRS (UJF, UPS, INSA), BP 166, 38042 Grenoble Cedex 9, France.
[6] Scientific-Practical Material Research Centre of the National Academy of Belarus, 19 P. Brovki, 220072 Minsk, Belarus.

Keywords $CuInTe_2$, Excitons, Magnetic field, Effective masses.

* Corresponding author: e-mail michael.yakushev@strath.ac.uk

$CuInTe_2$ single crystals were studied using optical magneto-reflectance (MR) in magnetic fields B up to 20 T at 4.2 K. The spectra exhibited the A and B free excitons blue shifting at increasing magnetic fields. Fitting quadratic functions to the experimental dependencies of the exciton spectral energy on B assuming a low-field limit allowed determination of diamagnetic shift rates of 8.2×10^{-5} eV/T^2 and 8.5×10^{-5} eV/T^2 for the A and B free excitons, respectively. Exciton reduced masses of $0.0575m_0$ and $0.0568m_0$ (m_0 is the free electron mass), Rydbergs of 6.2 meV and 6.1 meV, and Bohr radii 10.4 nm and 10.5 nm were then estimated. An electron effective mass of $0.062m_0$ and B sub-band effective hole mass of $0.70m_0$ were determined using a literature value of the A valence sub-band hole of $0.78m_0$.

1 Introduction

chalcopyrite compounds the alternation of two different cation atoms (Cu and In in the case of $CuInTe_2$) on the cation lattice induces a tetragonal distortion which splits the valence band of $CuInTe_2$ in the A, B and C sub-bands. For some chalcopyrites ($CuInSe_2$ and $CuGaSe_2$) an application in the absorber layer of thin film solar cells has been already found [2]. Their direct bandgaps (E_g) of 1 eV [3] and 1.7 eV [4], respectively, allow the bandgaps of their alloy $Cu(In,Ga)Se_2$ (CIGS) to be tuned to match the solar spectrum by changing the [Ga]/[Ga+In] ratio. An increase in the [Ga]/[Ga+In] ratio at first results in a rise of the open circuit voltage (V_{oc}) of CIGS-based solar cells. However, at [Ga]/[Ga+In] in excess of 0.3, the V_{oc} saturates developing a deficit which increases with rising gallium content [5]. This problem has not been solved as yet. The bandgap of $CuInTe_2$ of 1 eV is close to that of $CuInSe_2$ suggesting that $CuInTe_2$ can also be used in the absorber layer of thin film solar cells. Indeed, the conversion efficiency (η) of solar cells with $Cu(In,Ga)Te_2$ absorbers has already exceeded 4% [6]. However, this value is still below 22.9% [7], current η of $Cu(In,Ga)Se_2$-based photovoltaic (PV) devices. The electronic properties of $CuInTe_2$ are significantly less studied than those in $CuInSe_2$ and $CuGaSe_2$. A further progress in the development of $CuInTe_2$-based devices can be

should exhibit sharp excitonic features in their optical spectra which is possible at low defect concentrations [16].

$CuInTe_2$ belongs to a family of ternary semiconductors with chalcopyrite lattice structure [1]. Similar to other expected once understanding of the electronic properties of this material has become better.

Charge carrier effective masses are very important parameters of the electronic structure of semiconductors because such masses define the mobility of the carriers which, in turn, strongly influences the performance of electronic devices fabricated using these semiconductors [8]. A recent study of the electronic structure of $CuInTe_2$ carried out using angular resolved photoelectron spectroscopy demonstrated a remarkable steepness of the energy-momentum (E-k) dispersion relations of the valence band in this compound [9]. This can be very beneficial for solar cells based on this material.

Charge carrier masses reported for $CuInTe_2$ in the literature reveal a significant scatter. The hole effective mass varies from $2.2m_0$ [10] to $0.11m_0$ [11], where m_0 is the free electron mass, whereas that of the electron ranges from $0.058m_0$ [10] to $0.14m_0$ [12] or $0.155m_0$ [13].

Dispersion relations of the conduction and valence bands of semiconductors can also be examined by magneto-optical spectroscopy [14]. Such methods have been used to estimate reduced masses of free excitons in $CuInSe_2$ [15] and $CuGaSe_2$ [4]. A key requirement for the use of such techniques is a high structural quality of the examined materials. Such materials

In this report excitonic grade single crystals of $CuInTe_2$ (exhibiting excitons in their optical spectra) were examined by magneto-reflectance (MR) at 4.2 K and magnetic fields B up to 20 T.

2 Experimental

Single crystals of $CuInTe_2$ were grown using the vertical Bridgman technique [17,18]. Crystals from the middle part of the ingot were cleaved and then examined at zero magnetic fields for the presence of excitons in the photoluminescence (PL) and optical reflectance (OR) spectra. Such spectra, measured at liquid helium temperatures, were reported earlier [18]. The elemental composition of the samples was measured by wave-length dispersive spectrometry as Cu:25.4, In:25.3, and Te: 49.3 At.% corresponding to [Cu]/[In]=1.00 and [Te]/[Cu+In]=0.97. The samples were placed in the Faraday configuration (the sample surface being always perpendicular to the magnetic field direction ***B*** and the direction of the excitation light from a halogen tungsten lamp) into the bore of a 10 MW resistive magnet at the Grenoble High Magnetic Field Laboratory providing fields *B* up to 20 T. Light from the lamp was delivered to the samples by an optical fibre. Another fibre was used to collect the MR signal and deliver it to the slits of a 0.5 m focal length single grating (1800 grooves/mm) spectrometer with a liquid nitrogen cooled InGaAs array detector. The MR spectra were measured at a spectral resolution of 0.2 meV. The orientation of the lattice structure of the crystals with respect to the magnetic field direction was not examined. More details on the experimental set up can be found in ref. [4,15].

3 Results and discussions

OR spectra of $CuInTe_2$, measured at zero magnetic field and 4.2 K, exhibit two excitonic oscillations earlier assigned to the A and B free excitons at 1.053 eV and 1.072 eV, respectively [18]. These excitons are shown in **Figure 1(a)**.

The application of magnetic fields shifts both excitons towards higher energies. This shift can be seen in **Figure 1(b)**. It also can be seen that rising magnetic fields increase the magnitude of the oscillations of the A exciton. Each spectrum was fitted with the following function [19]:

$$R(E)=R_0+R_x(Re\{e^{i\theta}(E_x-E+i\Gamma_x)/[\Gamma_x^2+(E_x-E)^2]\}), \quad (1)$$

where E_x is the spectral energy of the A or B excitons, Γ_x is the broadening parameter, θ is the phase ($\theta_A=\theta_B$), R_x is an amplitude whereas R_0 is a background. An example of the fitting for the zero field spectrum is shown in **Figure 1(a)**. Such a fitting improved the accuracy of the determination of the spectral position of the excitons. Changes in the spectral position of the A and B excitons with increasing magnetic fields are shown in **Figure 2**.

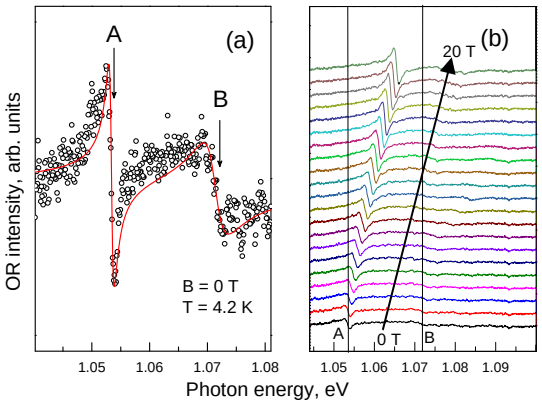

Figure 1 Experimental OR spectrum at zero magnetic field (◦), red solid line is the best fit (a), MR spectra at magnetic fields *B*, increasing from 0 T to 20 T (b).

The effect of the magnetic field depends on the balance of the strengths of the Lorentz and Coulomb forces. Weak fields do not break the Coulomb bond between the electron and hole but deform their relative motion making the originally *s*-type exciton wave-function slightly *p*-type [8]. As a result this wave-function acquires an angular momentum (l = 1) becoming proportional to *B*. Together with the magnetic dipole energy of the exciton, which is also proportional to *B*, the spectral energy of the exciton becomes quadratically dependent on *B*. Once the field becomes strong enough to break the Coulomb forces this quadratic dependence is substituted by a linear one. Thus, within weak magnetic field limits the dependence of the spectral energy *E(B)* of a free exciton on *B* can be described as the follows:

$$E(B) = E_0 + c_dB^2, \quad (2)$$

where E_0 is a zero field spectral energy and c_d is the rate of the shift called diamagnetic coefficient. This coefficient is proportional to the squared exciton wave-function and can be used to estimate the exciton size, the Bohr radius a_B [8].

Experimental points of the $E(B)$ dependence of the A and B excitons were fitted with the function in equation (2), gradually increasing the number of fitted points starting from 3. After each fitting the correlation coefficient R^2, reflecting the accuracy of the fit, was examined. Up to the fifth point (4 T) R^2 was increasing sharply. Further increases in the point number was rather marginal suggesting that at fields in excess of 4 T the dependence $E(B)$ admixes a linearity indicating the approach of the weak field limit when magnetic forces start breaking the Coulomb bonds [8].

The best fits and corresponding R^2 are shown in **Figure 2**. The diamagnetic shift rates c_d of (8.2 ± 0.3)×10^{-5} eV/T^2 for the A and (8.5 ± 0.4)×10^{-5} eV/T^2 for

the B excitons were determined. These shift rates are also shown in Table 1.

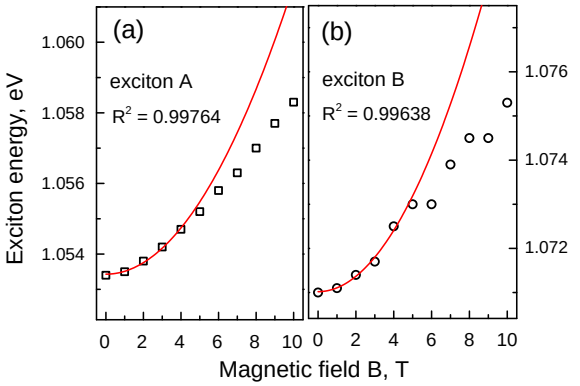

Figure 2 The dependence of the spectral position of the A (a) and B (b) free excitons on the magnetic field strength B (○). The red solid lines are best fits using quadratic functions.

A hydrogenic model for free Wannier excitons, neglecting the interaction between the A and B valence sub-bands, assuming isotropic parabolic valence and conduction bands, relates the diamagnetic spectral energy change ΔE_d induced by the influence of magnetic field with the Bohr radius a_B as follows [8]:

$$\Delta E_d = (e^2 a_B^2/4\mu)B^2, \qquad (3)$$

where $\mu = (1/m_e+1/m_h)^{-1}$ is the exciton reduced mass combining the electron m_e and hole m_h effective masses. Using $\varepsilon = 11.25$ [20] the average value of static dielectric constants along and perpendicular to the tetragonal axis in $CuInTe_2$, we determined reduced masses of the A and B excitons as $\mu_A = 0.0575m_0$ and $\mu_B = 0.0568m_0$, respectively (m_0 is the free electron mass). Effective Rydbergs of 6.2 meV and 6.1 meV for the A and B excitons, respectively, were also calculated using the following expression [8]:

$$Ry^* = 13.6\mu/(m_0\varepsilon^2), \qquad (4)$$

These Rydbergs are close to the A exciton binding energy of 6 meV, estimated as a difference between the spectral position of this exciton in the PL spectra (measured at 6 K) and E_g, determined by fitting theoretically calculated absorption spectra to experimental ones (also measured at 6 K) for the same sample [21,22]. Excitonic Bohr radii (a_B) of 10.4 nm and 10.5 nm, calculated for the A and B excitons, respectively, are shown in Table 1.

The scatter of reported effective masses for the A valence sub-band hole by more than an order of magnitude can be due to the differences in the quality of the examined materials. Some of the studied $CuInTe_2$ samples were polycrystalline films whereas others were single crystals of unknown crystalline quality. Effective masses of the A valence sub-band hole m_h(A), determined from infrared reflection spectra measured for oriented single crystals in ref. [23] and confirmed in ref.[24], are assumed to be more reliable. The average value of $0.78m_0$ for masses of $0.66m_0$ and $0.85m_0$, measured in ref.[23] for the electric field vector E parallel and perpendicular to the optical axis c, respectively, was used to calculate effective masses of the electron as $m_e = 0.062m_0$ and of the B valence sub-band hole as $m_h(B) = 0.70m_0$.

Table 1 Diamagnetic shift rates c_d, reduced masses μ, effective Rydbergs (Ry^*) and Bohr radii (a_B) of the A and B free excitons.

Band	c_d (eV/T^2)	μ (m_0)	Ry* (meV)	a_B (nm)
A	8.2×10^{-5}	0.0575	6.2	10.4
B	8.5×10^{-5}	0.0568	6.1	10.5

The diamagnetic shift rate determined here for the A exciton in $CuInTe_2$ (8.2×10^{-5} eV/T^2) is significantly greater than those reported for the better known chalcopyrites: $CuInSe_2$ (2.7×10^{-5} eV/T^2) [15], $CuGaSe_2$ (0.99×10^{-5} eV/T^2) [4] and $CuInS_2$ (0.46×10^{-5} eV/T^2) [16]. Because of this increased shift rate the size of the exciton in $CuInTe_2$, estimated by the Bohr radius of 10.4 nm, is twice as large as that of $CuInSe_2$, the nearest competitor amongst these compounds in terms of the diamagnetic shift rate magnitude with a_B of 5.1 nm [15]. The large diamagnetic shift rate and Bohr radius for the A exciton in $CuInTe_2$ result in the smallest reduced exciton mass of $\mu = 0.0575m_0$ ($0.081m_0$ [15] in $CuInSe_2$, $0.115m_0$ [4] in $CuGaSe_2$ and $0.141m_0$ [25] in $CuInS_2$) and effective electron mass ($0.09m_0$ [23] in $CuInSe_2$, $0.14m_0$ [4] in $CuGaSe_2$ and $0.16m_0$ in $CuInS_2$ [26]) amongst these chalcopyrite compounds. Such a lightness of the masses promises a high potential for the charge carrier mobility and consequently high potential performance of solar cells based on $CuInTe_2$. To compare electron effective masses as well as diamagnetic shift rates (c_d) and reduced masses (μ) of the A exciton in $CuInTe_2$, $CuInSe_2$, $CuGaSe_2$ and $CuInS_2$ we collected these values in Table 2.

4 Conclusion

High structural quality single crystals of $CuInTe_2$ were studied by MR at 4.2 K in magnetic fields B up to 20 T. Zero field OR spectra of the crystals revealed A and B free excitons. The spectral energies of these excitons demonstrated significant blue shifts at increasing magnetic fields. Diamagnetic coefficients of 8.2×10^{-5} eV/T^2 and 8.5×10^{-5} eV/T^2 for the A and B free

excitons, respectively, were determined by fitting quadratic functions into the experimental points assuming a low-field limit. Exciton reduced masses of $0.0575m_0$ and $0.0568m_0$, Rydbergs of 6.2 meV and 6.1 meV, Bohr radii 10.4 nm and 10.5 nm, were calculated applying an isotropic hydrogenic model of a free Wannier exciton in magnetic fields. An effective mass of the electron of $0.062m_0$ and B sub-band hole mass of $0.70m_0$ were calculated assuming a literature A sub-band hole mass of $0.78m_0$.

Table 2 A comparison of electron effective masses (m_e), diamagnetic shift rates (c_d) and reduced masses (μ) of the A exciton in $CuInTe_2$, $CuInSe_2$, $CuGaSe_2$ and $CuInS_2$.

Material	m_e (m_0)	c_d (eV/T^2)	μ (m_0)
$CuInTe_2$	0.062	8.2×10^{-5}	0.0575
$CuInSe_2$	0.09	2.7×10^{-5}	0.081
$CuGaSe_2$	0.14	0.99×10^{-5}	0.115
$CuInS_2$	0.16	0.46×10^{-5}	0.141

Acknowledgements The study was supported by the Russian Science Foundation (grant 17-12-01500) and LNCMI-CNRS (EMFL).

References

[1] J.L. Shay, J.H. Wernick, Ternary Chalcopyrite Semiconductors. Growth, Electronic Properties and Applications. Pergamon, New York (1975). p. 254.
[2] M.A. Green, Y. Hishikawa, E.D. Dunlop, D.H. Levi, J. Hohl-Ebinger, A.W.Y. ho-Baillie. Prog. Photovolt. Res. Appl. 26, 3 (2018).
[3] M.V. Yakushev, F. Luckert, C. Faugeras, A. V. Karotki, A.V. Mudryi,and R.W. Martin, Appl. Phys. Lett. **97**, 152110 (2010).
[4] F. Luckert, M. V. Yakushev, C. Faugeras, A. V. Karotki, A. V. Mudryi, and R. W. Martin, Appl. Phys. Lett. **97**, 162101 (2010).
[5] M. A. Contreras, L. M. Mansfield, B. Egaas, J. Li, M. Romero, R. Noufi, E. Rudiger-Voigt and W. Mannstadt, Prog. Photovolt: Res. Appl. **20**, 843 (2012).
[6] M. Lakhe, N.B. Chaure, Solar Energy Materials and Solar Cells **123**, 122 (2014).
[7] T. Kato, J.-L. Wu, Y. Hirai, H. Sugimoto, and V. Bermudez, IEEE Journal of Photovoltaics **9**, 325 (2019).
[8] C.F. Klingshirn, *Semiconductor Optics*. Springer-Verlag, Berlin, Heidelberg **2005**, p. 797.
[9] J.J. Frick, A. Topp, S. Klemenz, M.S. Krivenkov, A.Y. Varykhalov, C. Ast, A.B. Bocarsly, L.M. Schoop, J. Phys. Chem. Lett. **9**, 6833 (2018).
[10] L.I. Berger & V.M.Petrov, Izv. Akad. Nauk SSSR Neorg. Mater. **6**, 1348 (1970).
[11] S. M. Wasim, G. Marcano, and G. S. Porras, Jpn. J. Appl. Phys. Suppl. **19-3**, 133 (1980).
[12] S.M. Wasim, Phys. Status Solidi A **75**, K69 (1983).
[13] S. M. Wasim and J. G. Albornoz, Phys. Status Solidi A **110**, 575 (1988).
[14] J.O. Dimmock and R.G. Weeler, J. Appl. Phys. **32**, 2271 (1961).
[15] M.V. Yakushev, F.Luckert, A.V. Rodina, C.Faugeras, A.V. Mudryi, A.V.Karotki and R.W. Martin, Appl. Phys. Lett. 101, 262101 (2012).
[16] E.H. Bogardus, H.B. Bebb, Phys. Rev. **176**, 993 (1968).
[17] R.D. Tomlinson, Solar Cells 16, 17 (1986).
[18] M.V. Yakushev, A.V. Mudryi, E. Kärber, P.R. Edwards and R.W. Martin, Appl. Phys. Lett. **114**, 062103 (2019).
[19] K.P. Korona, A. Wysmołek, K. Pakuła, R. Stepniewski, J. M. Baranowski, I. Grzegory, B. Łucznik, M. Wroblewski, and S. Porowski, Appl. Phys. Lett. **69**, 788 (1996).
[20] V. Riede, H. Neumann, H. Sobotta, R.D. Tomlinson, E. Elliott, & L. Howarth, Solid State Commun. **33**, 557 (1980).
[21] G. Marın, C. Rincon, S. M. Wasim, Ch. Power, and G. S. Perez, J. Appl. Phys. **81**, 7580 (1997).
[22] C. Rincón, S. M. Wasim, G. Marín, G. Sánchez Pérez, and G. Bacquet, J. Appl. Phys. **82**, 4500 (1997).
[23] H. Weinert, H. Neumann, H. J. Hobler, G. Kuhn, N. V. Nam, Phys. Status Solidi B **81**, K29 (1977).
[24] G. Marin, S. M. Wasim, G. Sánchez Pérez, P. Bocaranda, A. E. Mora, J. Electronic Materials, **27**, 1351 (1998).
[25] M.V. Yakushev, R.W. Martin and A.V. Mudryi, Appl. Phys. Lett. **94**, 042109 (2009).
[26] D.C. Look, T.C. Manthuruthil, J. Phys. Chem. Sol. **37**, 173 (1976).